Acoustic and Electromagnetic Wave Interaction: Analytical Formulation for Acousto-Electromagnetic Scattering Behavior of a Dielectric Cylinder

Daniel E. Lawrence, *Student Member, IEEE,* and Kamal Sarabandi, *Fellow, IEEE*

***Abstract*—An analytical solution for the bi-static electromagnetic (EM) scattering from an acoustically excited vibrating dielectric circular cylinder is presented. The incident acoustic wave causes a boundary deformation as well as a dielectric inhomogeneity within the dielectric cylinder. First, a perturbation method is developed to calculate the EM scattering from a slightly deformed and inhomogeneous dielectric cylinder. Then, assuming the vibration frequency is much smaller than the frequency of the incident EM wave, a closed form expression for the time-frequency response of the bi-static scattered field is obtained. The solution for acoustic scattering from an elastic cylinder is applied to give the displacement on the surface as well as the compression and dilation within the cylinder. Both the surface displacement and the variation in material density (dielectric constant fluctuation) within the cylinder contribute to the Doppler component of the EM scattered field. Results indicate that the Doppler frequencies correspond to the mechanical vibration frequencies of the cylinder and that the Doppler components only become sizeable near frequencies corresponding to the natural modes of free vibration in the cylinder. These resonances depend only on the object properties and are independent of the surrounding medium. Thus, utilizing the information in the Doppler spectrum scattered by an acoustically excited object vibrating at resonance could provide a means for buried object identification.**

***Index Terms*—Acoustics, Doppler spectra, electromagnetic scattering, perturbation techniques.**

I. Introduction

GROUND penetrating radars (GPR) have been proposed for the detection and identification of buried objects [1]. Applications of GPR include the detection of buried pipes and cables, unexploded ordnance (UXO) detection, and both military and humanitarian demining. The ability of GPR to detect some buried objects is severely limited by the low dielectric contrast between buried objects and the soil background. This is especially true for antipersonnel (AP) landmines, which are composed mostly of plastic. In order to increase the probability of detection without increasing the false alarm rate, measurable quantities that are characteristic of the objects of interest should be exploited. One such quantity is the electromagnetic (EM) Doppler spectrum scattered from an object being mechanically vibrated by an incident acoustic wave. As proposed in an earlier work by the authors [2], the acoustically induced Doppler spectra scattered from a buried object could be used as a means for buried object detection/discrimination.

The idea of EM scattering combined with acoustic excitation for detecting buried objects has been addressed previously [3], [4]. Experimental results are reported in [5] and [6], where an EM radar is used to measure surface displacement caused by a traveling surface acoustic wave. In this approach, object detection is based on the small changes in surface displacement when a buried object is introduced. Other experimental results are reported in [7] where mechanical excitation is achieved through high-pressure water jets. In this technique, both acoustic and EM receivers are used to detect ground vibrations. To aid in clutter rejection, however, distinguishing characteristics of the objects of interest, such as the normal modes of free vibration, should be incorporated into the detection scheme. In this paper, the phenomenology associated with the scattered Doppler spectrum from an acoustically vibrated object is examined as a possible means of target identification. The proposed detection and identification scheme is shown in Fig. 1.

Before an acousto-electromagnetic detection scheme can be effective, the relationship between the vibrating mechanical modes of an object and the scattered Doppler spectrum must be understood. In [2], an analytical solution for the Doppler scattering from a perfectly conducting circular cylinder in air was formulated and the current paper will extend these results to a solid dielectric circular cylinder. One of the simplest scattering problems (acoustic or EM) for which an exact solution exists involves an infinitely long circular cylinder in a homogeneous background. An infinite cylinder provides an accurate model for buried pipes and cables but is admittedly not particularly descriptive of landmines. The purpose of this paper, however, is not to develop scattering models for specific landmines, but instead to demonstrate the phenomena associated with the acousto-electromagnetic scattering behavior of dielectric objects in general. In this respect, the two-dimensional (2-D) nature of the cylinder makes it a good candidate for a phenomenology study without unduly complicating the mathematics.

A vibrating dielectric cylinder exhibits two sources of Doppler scattering: the cylinder shape variation and the dielectric constant fluctuation within the cylinder. As the incident acoustic wave vibrates the cylinder, both the cylinder's shape and density profile within the cylinder vary with time. Hence, the EM scattering solution for an arbitrarily deformed, inhomogeneous dielectric cylinder is needed. Numerical techniques could be employed to calculate the scattering from a deformed

Manuscript received February 28, 2001; revised August 16, 2000.

The authors are with the Radiation Laboratory, Department of Electrical Engineering and Computer Science, The University of Michigan, Ann Arbor, MI 48109-2122 USA (e-mail: delawren@eecs.umich.edu; saraband@eecs.umich.edu).

Publisher Item Identifier S 0018-926X(01)07647-5.

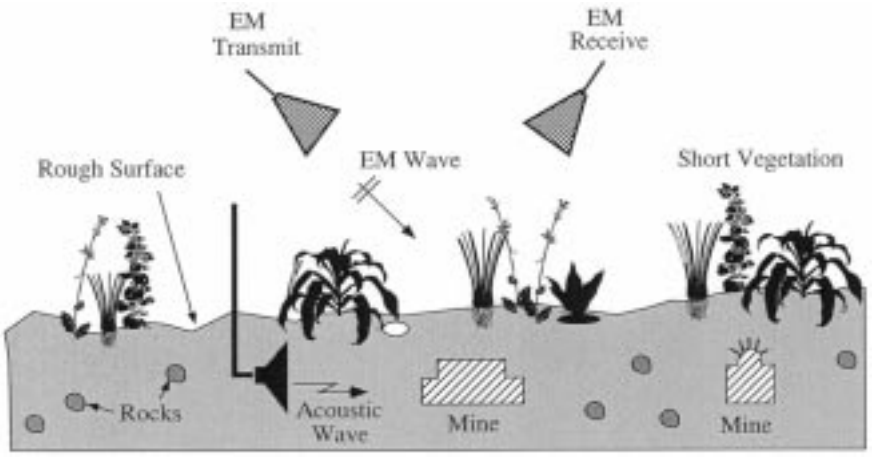

Fig. 1. Example scenario for acousto-electromagnetic object detection.

cylinder [8], but the acoustic induced vibrations considered in the current paper are generally very small compared to the EM wavelength and would require an impractically large number of discretization points on the object. For example, at an acoustic resonance the maximum displacement for the cylinder considered in Section III is on the order of $10^{-4}\lambda$. Consequently, analytical perturbation techniques were chosen to calculate the scattered fields. Perturbation techniques can provide analytical solutions to problems when the surface irregularity and dielectric inhomogeneity are small and exact solutions exist for the unperturbed problems. Perturbation theory is an established analytical approach for scattering solutions and was applied by Rayleigh [9] and Maxwell [10], to certain scalar field problems. These methods have found application in EM scattering from rough surfaces [11], [12] cylinders [13]–[15], and spheres [16], [17]. In the current paper, the scattering contribution from the boundary deformation is obtained through a perturbation expansion of the exact eigenfunction solution for a homogeneous dielectric cylinder. Yeh [14] presents a methodology for this approach and derives the perturbation coefficients for the specific case of a dielectric elliptic cylinder with small eccentricity. For the present work, however, the (time-varying) perturbation coefficients for an arbitrarily deformed dielectric cylinder are needed and will be derived using a similar approach. The contribution from the dielectric fluctuation is formulated by expanding the interior fields in terms of a perturbation parameter related to the dielectric inhomogeneity and then using the induced volumetric current to calculate the scattered field. This method is simply an application of the well known Born approximation described in [18]. It has been applied to scattering from inhomogeneous dielectric rough surfaces [19] and from low contrast, buried dielectric cylinders [20]. To the best of the authors' knowledge, application of this approach to an inhomogeneous dielectric cylinder has not previously been done.

Assuming the acoustic vibration frequency to be much smaller than the EM frequency, a Fourier transform can be used to extract the Doppler spectrum from the time-varying deformed and inhomogeneous dielectric cylinder. The time-varying displacement on the surface and within the cylinder is obtained from the analytical solution for the acoustic scattering from a solid elastic cylinder. Several examples are presented to illustrate the relationship between the scattered Doppler spectrum and the acoustic resonances of a dielectric cylinder. As will be shown, the bistatic Doppler spectrum provides a means for noninvasive measuring of the mechanical vibration modes of an object. Furthermore, the effect of EM resonances in the scattered Doppler spectrum will be examined.

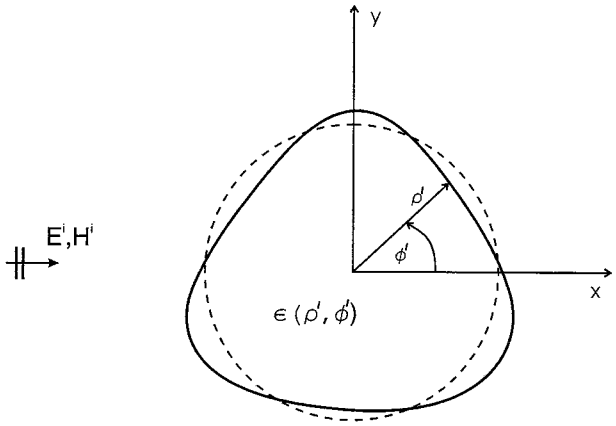

Fig. 2. Geometry for EM scattering of a plane wave from a dielectric cylinder whose shape and dielectric constant profile are perturbed.

II. Analytical Development

A. TM Case

1) Shape Perturbation: Following the methodology presented in [14], an analytical solution for the EM scattering from a slightly deformed dielectric circular cylinder is derived using a perturbation method. Consider a plane wave incident upon a perturbed dielectric cylinder as shown in Fig. 2. The radius of the cylinder can be expressed in polar coordinates as,

$$\rho' = a + bf(\phi', t) \tag{1}$$

where

a	unperturbed radius;
$f(\phi', t)$	periodic and smooth function of ϕ';
b	perturbation parameter assumed to be much smaller than the wavelength and the radius a.

The standard method for calculating the scattered field from a dielectric cylinder is the eigenfunction expansion of the total field. From the development in [21], consider an incident TM plane wave propagating along the $+x$-direction with a polarization parallel to the cylinder's axis expressed as

$$E_z^i = e^{-jk_0\rho\cos\phi} = \sum_{n=-\infty}^{\infty} j^{-n} J_n(k_0\rho) e^{jn\phi} \tag{2}$$

where k_0 is the wavenumber in free space. When there is no perturbation on the surface (i.e., $b = 0$), the scattered field external to the cylinder is given by

$$E_z^s = \sum_{n=-\infty}^{\infty} j^{-n} A_n^{\mathrm{TM}} H_n^{(2)}(k_0\rho) e^{jn\phi} \tag{3}$$

with

$$A_n^{\mathrm{TM}} = \frac{\dfrac{\eta_0}{\eta_d} J_n(k_0a) J_n'(k_da) - J_n'(k_0a) J_n(k_da)}{J_n(k_da) H_n^{(2)\prime}(k_0a) - \dfrac{\eta_0}{\eta_d} J_n'(k_da) H_n^{(2)}(k_0a)} \tag{4}$$

where η_0 and η_d are the wave impedances in free space and within the dielectric, respectively, and k_d is the wavenumber in the dielectric. The scattered field internal to the cylinder is

$$E_z^{sd} = \sum_{n=-\infty}^{\infty} j^{-n} B_n^{\mathrm{TM}} J_n(k_d\rho) e^{jn\phi} \tag{5}$$

with

$$B_n^{\mathrm{TM}} = \frac{-2j/\pi k_0 a}{J_n(k_da) H_n^{(2)\prime}(k_0a) - \dfrac{\eta_0}{\eta_d} J_n'(k_da) H_n^{(2)}(k_0a)}. \tag{6}$$

Now, if a small perturbation is introduced on the boundary, the scattered fields can be expanded in a perturbation series in k_0b and k_db, respectively. To the first order in k_0b, we may express the external field

$$E_z^s = \sum_{n=-\infty}^{\infty} j^{-n} A_n^{\mathrm{TM}} (1 + C_n^{\mathrm{TM}} k_0 b) H_n^{(2)}(k_0\rho) e^{jn\phi} \tag{7}$$

and the internal field to the first order in k_db

$$E_z^{sd} = \sum_{n=-\infty}^{\infty} j^{-n} B_n^{\mathrm{TM}} (1 + D_n^{\mathrm{TM}} k_d b) J_n(k_d\rho) e^{jn\phi} \tag{8}$$

where C_n^{TM} and D_n^{TM} are unknown coefficients to be determined from the boundary conditions at the surface of the perturbed cylinder. The boundary conditions mandate that the tangential electric and magnetic fields be continuous at the surface of the cylinder. Note that the unit vector tangent to the perturbed cylinder surface can be written

$$\hat{u}_t = \alpha[\beta\hat{u}_\rho + \hat{u}_\phi]$$

where

α	$= \{[bf'(\phi', t))/(a + bf(\phi', t))]^2 + 1\}^{-1/2}$;
β	$= bf'(\phi', t)/(a + bf(\phi', t))$;
$f'(\phi', t)$	partial derivative of $f(\phi', t)$ with respect to ϕ'.

The tangential magnetic fields on the surface of the perturbed cylinder for the incident, external scattered, and internal scattered fields are given, respectively, by

$$H_{\tan}^i = \frac{j}{\eta_0} \sum_{n=-\infty}^{\infty} \alpha j^{-n} \left[\frac{\beta jn}{k_0\rho'} J_n(k_0\rho') - J_n'(k_0\rho')\right] e^{jn\phi'} \tag{9}$$

$$H_{\tan}^s = \frac{j}{\eta_0} \sum_{n=-\infty}^{\infty} \alpha j^{-n} A_n^{\mathrm{TM}} (1 + C_n^{\mathrm{TM}} k_0 b) \cdot \left[\frac{\beta jn}{k_0\rho'} H_n^{(2)}(k_0\rho') - H_n^{(2)\prime}(k_0\rho')\right] e^{jn\phi'} \tag{10}$$

$$H_{\tan}^{sd} = \frac{j}{\eta_d} \sum_{n=-\infty}^{\infty} \alpha j^{-n} B_n^{\mathrm{TM}} (1 + D_n^{\mathrm{TM}} k_d b) \cdot \left[\frac{\beta jn}{k_d\rho'} J_n(k_d\rho') - J_n'(k_d\rho')\right] e^{jn\phi'}. \tag{11}$$

Using Taylor series expansion, the eigenfunctions in the above expressions can be approximated to the first order in k_0b and k_db, and are given in general by

$$Z_n(k\rho') = Z_n(k[a + bf(\phi')]) \approx Z_n(ka) + kbf(\phi', t) Z_n'(ka) \tag{12}$$

where Z_n represents the Bessel or Hankel function of nth order (or their derivatives) and k represents either k_0 or k_d accordingly. Also expanding α, β, and ρ' in (2), (7)–(11) and keeping terms up to first order in kb, two equations result for the perturbation coefficients C_n^{TM} and D_n^{TM} by applying the boundary conditions at the surface of the perturbed cylinder. These equations are solved by expanding $f(\phi', t)$ in terms of a Fourier series with respect to ϕ' with the pth Fourier series coefficient denoted $f_p(t)$

$$f(\phi', t) = \sum_{p=-\infty}^{\infty} f_p(t) e^{jp\phi'}. \tag{13}$$

The explicit form for C_n^{TM} is found to be

$$C_n^{\mathrm{TM}}(t) = \frac{j^n J_n(k_da) \displaystyle\sum_{p=-\infty}^{\infty} f_{n-p}(t) V_p}{\dfrac{\eta_0}{\eta_d} J_n(k_0a) J_n'(k_da) - J_n'(k_0a) J_n(k_da)} \tag{14}$$

where

$$V_p = j^{-p}\left[-J_p''(k_0a) - A_p^{\mathrm{TM}} H_p^{(2)\prime\prime}(k_0a) + \frac{k_d^2}{k_0^2} B_p^{\mathrm{TM}} J_p''(k_da)\right].$$

The expression in (14) provides the TM solution for the scattered field from a homogeneous dielectric cylinder with a perturbed cross section.

2) Dielectric Perturbation: A vibrating cylinder that is initially homogeneous will experience density fluctuations as the cylinder vibrates. As a result, the dielectric constant will fluctuate within the cylinder requiring a solution for the EM scattering from a slightly inhomogeneous dielectric cylinder. Since the dielectric fluctuations are small, we will once again develop a perturbation technique to solve for the scattered fields. The

technique presented here is similar to that used for scattering from a low contrast dielectric cylinder given in [20]. The dielectric constant of the cylinder can be written

$$\epsilon(\rho', \phi', t) = \epsilon_d + \delta\tilde{\epsilon}(\rho', \phi', t) \tag{15}$$

where δ is a perturbation parameter assumed to be small (i.e., $\delta \ll 1$). Gauss' law in a source free region asserts

$$\nabla \cdot [\epsilon(\rho', \phi', t)\mathbf{E}] = \epsilon(\rho', \phi', t)\nabla \cdot \mathbf{E} + \nabla\epsilon(\rho', \phi', t) \cdot \mathbf{E} = 0.$$

Which indicates

$$\nabla \cdot \mathbf{E} = -\frac{1}{\epsilon(\rho', \phi', t)} \nabla\epsilon(\rho', \phi', t) \cdot \mathbf{E}.$$

Since $\nabla\epsilon(\rho', \phi', t)$ does not contain a z-component and the electric field has only a z-component for the TM case, we conclude that

$$\nabla \cdot \mathbf{E} = 0.$$

Now it can be easily shown from Maxwell's equations that the wave equation for E_z can be written

$$\nabla^2 E_z + \omega^2\mu\epsilon_0 E_z = 0 \qquad \text{external to cylinder} \tag{16}$$

$$\nabla^2 E_z + \omega^2\mu\epsilon(\rho', \phi', t)E_z = 0 \qquad \text{internal to cylinder.} \tag{17}$$

Substituting the perturbation expression from (15) into (17) gives

$$\nabla^2 E_z + k_d^2 E_z = -\omega^2\mu\delta\tilde{\epsilon}(\rho', \phi', t)E_z \tag{18}$$

where $k_d^2 = \omega^2\mu\epsilon_d$. Since δ is small, E_z can be expanded in a convergent perturbation series in δ, and is given by

$$E_z = \sum_{n=0}^{\infty} E_z^{(n)}\delta^n \tag{19}$$

where $E_z^{(0)}$ is the scattered field from the unperturbed cylinder. Substituting (19) into (18) and collecting equal powers of δ, it can be easily shown that

$$\nabla^2 E_z^{(n)} + k_d^2 E_z^{(n)} = -\omega^2\mu\tilde{\epsilon}(\rho', \phi', t)E_z^{(n-1)}. \tag{20}$$

Hence, the $(n-1)$th-order solution acts as the source function for the nth-order solution. Now, the first-order scattered field external to the cylinder can be obtained by

$$E_z^{(1)} = -\omega^2\mu \int_0^{2\pi}\int_0^a \tilde{\epsilon}(\rho', \phi', t)E_z^{(0)} \cdot G(\rho, \rho', \phi, \phi')\rho'\, d\rho'\, d\phi' \tag{21}$$

where $G(\rho, \rho', \phi, \phi')$ is the Green's function for a source internal to the cylinder and the observation external to the cylinder. After some lengthy manipulation, this Green's function can be shown to be [22]

$$G(\rho, \rho', \phi, \phi') = \sum_{m=-\infty}^{\infty} X_m J_m(k_d\rho')H_m^{(2)}(k_0\rho)e^{jm(\phi-\phi')} \tag{22}$$

where

$$X_m = \frac{1}{2\pi k_0 a} \cdot \left[\frac{1}{J_m(k_d a)H_m^{(2)\prime}(k_0 a) - \dfrac{\eta_0}{\eta_d} J_m'(k_d a)H_m^{(2)}(k_0 a)}\right].$$

Substituting (22) and the unperturbed scattered field from (5) for $E_z^{(0)}$ in (21) and simplifying gives

$$E_z^{(1)} = 2\pi\omega^2\mu \sum_{m=-\infty}^{\infty} X_m H_m^{(2)}(k_0\rho)e^{jm\phi} \sum_{n=-\infty}^{\infty} j^{-n}B_n^{\mathrm{TM}} \cdot \int_0^a \tilde{\epsilon}_{n-m}(\rho', t)J_n(k_d\rho')J_m(k_d\rho')\rho'\, d\rho' \tag{23}$$

where $\tilde{\epsilon}_{n-m}(\rho', t)$ is the $(n-m)$th Fourier series coefficient of $\tilde{\epsilon}(\rho', \phi', t)$ when expanded in a Fourier series in ϕ'. This expression provides the TM solution for the first order scattered fields from an inhomogeneous dielectric cylinder.

B. TE Case

1) Shape Perturbation: Similar to the TM case, the EM scattering from a slightly deformed dielectric cylinder with a TE incident plane is derived using the perturbation method. The radius of the deformed cylinder is given in (1). The incident magnetic field can be expressed as

$$H_z^i = e^{-jk_0\rho\cos\phi} = \sum_{n=-\infty}^{\infty} j^{-n}J_n(k_0\rho)e^{jn\phi}. \tag{24}$$

The unperturbed scattered fields are given in (3) and (5) with E_z replaced by H_z, and the coefficients A_n^{TE} and B_n^{TE} are given in (4) and (6) with an interchange of η_0 and η_d. When a small perturbation is introduced on the boundary, the perturbed fields can be expanded in a perturbation series in $k_0 b$ and $k_d b$, respectively. The external field is given by

$$H_z^s = \sum_{n=-\infty}^{\infty} j^{-n}A_n^{\mathrm{TE}}(1 + C_n^{\mathrm{TE}}k_0 b)H_n^{(2)}(k_0\rho)e^{jn\phi} \tag{25}$$

and the internal field

$$H_z^{sd} = \sum_{n=-\infty}^{\infty} j^{-n}B_n^{\mathrm{TE}}(1 + D_n^{\mathrm{TE}}k_d b)J_n(k_d\rho)e^{jn\phi}. \tag{26}$$

The unknown coefficients, C_n^{TE} and D_n^{TE}, are to be determined from the boundary conditions applied at the surface of the perturbed cylinder. The boundary conditions specify that the total tangential electric and magnetic fields be continuous at the cylinder boundary. The tangential electric fields on the surface of the perturbed cylinder for the incident, external scattered, and internal scattered fields are given, respectively, by

$$E_{\tan}^i = \frac{j}{\eta_0} \sum_{n=-\infty}^{\infty} \alpha j^{-n}\left[\frac{\beta jn}{k_0\rho'}J_n(k_0\rho') - J_n'(k_0\rho')\right]e^{jn\phi'} \tag{27}$$

$$E_{\tan}^s = \frac{j}{\eta_0} \sum_{n=-\infty}^{\infty} \alpha j^{-n}A_n^{\mathrm{TE}}(1 + C_n^{\mathrm{TE}}k_0 b) \cdot \left[\frac{\beta jn}{k_0\rho'}H_n^{(2)}(k_0\rho') - H_n^{(2)\prime}(k_0\rho')\right]e^{jn\phi'} \tag{28}$$

$$E_{\tan}^{sd} = \frac{j}{\eta_d} \sum_{n=-\infty}^{\infty} \alpha j^{-n} B_n^{\mathrm{TE}} (1 + D_n^{\mathrm{TE}} k_d b) \cdot \left[\frac{\beta j n}{k_d \rho'} J_n(k_d \rho') - J_n'(k_d \rho') \right] e^{jn\phi'}. \quad (29)$$

Using the Taylor series expansions in (12) for the Bessel and Hankel functions and applying the boundary conditions results in two equations for the unknown coefficients C_n^{TE} and D_n^{TE}. Expanding $f(\phi', t)$ in a Fourier series as in (13), neglecting terms containing $(kb)^2$ and higher, and solving for C_n^{TE} completes the solution for the TE solution for the boundary perturbation

$$C_n^{\mathrm{TE}}(t) = \frac{j^n \sum_{p=-\infty}^{\infty} f_{n-p}(t) \left[\frac{\eta_0}{\eta_d} J_n(k_d a) V_{p,n-p} - J_n'(k_d a) U_p \right]}{J_n(k_0 a) J_n'(k_d a) - \frac{\eta_0}{\eta_d} J_n'(k_0 a) J_n(k_d a)} \quad (30)$$

where

$$V_{p,n-p} = j^{-p} \left[\frac{-p(n-p)}{(k_0 a)^2} B_p^{\mathrm{TE}} J_p(k_d a) \left(1 - \frac{\epsilon_0}{\epsilon_d} \right) - J_p''(k_0 a) - A_p^{\mathrm{TE}} H_p^{(2)\prime\prime}(k_0 a) + B_p^{\mathrm{TE}} J_p''(k_d a) \right]$$

and

$$U_p = j^{-p} \left[\frac{k_d}{k_0} B_p^{\mathrm{TE}} J_p'(k_d a) - A_p^{\mathrm{TE}} H_p^{(2)\prime}(k_0 a) - J_p'(k_0 a) \right].$$

2) Dielectric Perturbation: As with the TM case, the dielectric fluctuation induced by the mechanical vibration of the cylinder will contribute to the scattered field. The dielectric constant internal to the cylinder is again expressed by (15). The curl of Ampére's law, extended to the time-varying case, in a source free region is given by

$$\nabla \times \nabla \times \mathbf{H} = j\omega \nabla \times [\epsilon(\rho', \phi', t)\mathbf{E}] \quad (31)$$

$$= j\omega \nabla \epsilon(\rho', \phi', t) \times \mathbf{E} + j\omega \epsilon(\rho', \phi', t) \nabla \times \mathbf{E}. \quad (32)$$

It can easily be shown from Maxwell's equations that the wave equation for H_z is

$$\nabla^2 H_z + \omega^2 \mu \epsilon_0 H_z = 0 \quad \text{external to cylinder} \quad (33)$$

$$\nabla^2 H_z + \omega^2 \mu \epsilon(\rho', \phi', t) H_z = [-j\omega \nabla \epsilon(\rho', \phi', t) \times \mathbf{E}]_z \quad \text{internal to cylinder.} \quad (34)$$

Substituting (15) in (34) results in

$$\nabla^2 H_z + k_d^2 H_z = [-j\omega \nabla \delta \tilde{\epsilon}(\rho', \phi', t) \times \mathbf{E}]_z - \omega^2 \mu \delta \tilde{\epsilon}(\rho', \phi', t) H_z. \quad (35)$$

Since δ is small, both H_z and $\mathbf{E}$ will be expanded in a perturbation series in δ

$$H_z = \sum_{n=0}^{\infty} H_z^{(n)} \delta^n \quad \text{and} \quad \mathbf{E} = \sum_{n=0}^{\infty} \mathbf{E}^{(n)} \delta^n. \quad (36)$$

Substituting (36) into (35) and equating equal powers of δ, it can easily be shown that

$$\nabla^2 H_z^{(n)} + k_d^2 H_z^{(n)} = [-j\omega \nabla \tilde{\epsilon}(\rho', \phi', t) \times \mathbf{E}^{(n-1)}]_z - \omega^2 \mu \tilde{\epsilon}(\rho', \phi', t) H_z^{(n-1)}. \quad (37)$$

Here the $(n-1)$th order solution generates the source function for the nth order solution. The first order scattered field external to the cylinder can be obtained by

$$H_z^{(1)} = \int_0^{2\pi} \int_0^a \left\{ \left[-j\omega \nabla \tilde{\epsilon}(\rho', \phi', t) \times \mathbf{E}^{(0)} \right]_z - \omega^2 \mu \tilde{\epsilon}(\rho', \phi', t) H_z^{(0)} \right\} \cdot G^{\mathrm{TE}}(\rho, \rho', \phi, \phi') \rho' \, d\rho' \, d\phi' \quad (38)$$

where $G^{\mathrm{TE}}(\rho, \rho', \phi, \phi')$ is the Green's function for the TE case with a source internal to the cylinder and the observation external to the cylinder. From [22], this Green's function can be shown to be

$$G^{\mathrm{TE}}(\rho, \rho', \phi, \phi') = \sum_{m=-\infty}^{\infty} Y_m J_m(k_d \rho') \cdot H_m^{(2)}(k_0 \rho) e^{jm(\phi - \phi')} \quad (39)$$

where

$$Y_m = \frac{1}{2\pi k_0 a} \cdot \left[\frac{1}{J_m(k_d a) H_m^{(2)\prime}(k_0 a) - \frac{\eta_d}{\eta_0} J_m'(k_d a) H_m^{(2)}(k_0 a)} \right].$$

Substituting (39) and the unperturbed internal scattered fields into (38) simplifies to

$$H_z^{(1)} = 2\pi \sum_{m=-\infty}^{\infty} Y_m H_m^{(2)}(k_0 \rho) e^{jm\phi} \sum_{n=-\infty}^{\infty} j^{-n} B_n^{\mathrm{TE}} I_{m,n} \quad (40)$$

where

$$I_{m,n} = \int_{\rho'=0}^{a} \left\{ \left[\frac{n(m-n)}{\rho' 2} + k_d^2 \right] J_n(k_d \rho') \tilde{\epsilon}_{m-n}(\rho', t) - k_d J_n'(k_d \rho') \frac{\partial}{\partial \rho'} \tilde{\epsilon}_{m-n}(\rho', t) \right\} \cdot \frac{J_m(k_d \rho')}{\epsilon_d} \rho' \, d\rho'$$

and $\tilde{\epsilon}_{m-n}(\rho', t)$ is the $(m-n)$th Fourier series coefficient when $\tilde{\epsilon}(\rho', \phi', t)$ is expanded in a Fourier series in ϕ'.

C. Acoustic Vibration

In order to calculate the scattered fields from an acoustically vibrated cylinder, the boundary and dielectric fluctuations of the cylinder due to the acoustic excitation must be known. A thorough treatment of the acoustic scattering of an incident plane wave from a solid cylinder is given in [23]. Inherent in this formulation is the resulting mechanical vibration, which is of interest to us. Both the surface displacement and interior displacement of the cylinder are completely described by the displacement vector, $\mathbf{u}(\rho', \phi', t)$ whose components are of the form [23]

$$u_\rho = \sum_{n=0}^{\infty} \left[\frac{n b_n}{\rho} J_n(\kappa_2 \rho) - a_n \frac{d}{d\rho} J_n(\kappa_1 \rho) \right] \cos n\phi \quad (41)$$

$$u_\phi = \sum_{n=0}^{\infty} \left[\frac{n a_n}{\rho} J_n(\kappa_1 \rho) - b_n \frac{d}{d\rho} J_n(\kappa_2 \rho) \right] \sin n\phi \quad (42)$$

with the harmonic time dependence $e^{j\omega_a t}$ suppressed. The acoustic vibration frequency is denoted ω_a, the propagation constants κ_1 and κ_2 are for the compressional wave and shear wave within the cylinder, respectively, and the coefficients a_n and b_n contain rather lengthy expressions and can be found in [2, Appendix]. For the cylinder shape variation, the cylinder's radial displacement at the surface depends on both $u_\rho(a, \phi', t)$ and $u_\phi(a, \phi', t)$ but can be set equal to $u_\rho(a, \phi', t)$ to the first order. Thus, the displacement from (1) can be written

$$bf(\phi', t) = u_\rho(a, \phi', t). \tag{43}$$

Rewriting u_ρ with the time dependence explicitly shown

$$u_\rho(a, \phi', t) = \sum_{n=0}^{\infty} \Gamma_n \cos(\omega_a t + \theta_n) \cos n\phi' \tag{44}$$

where Γ_n and θ_n are the magnitude and phase, respectively, of the coefficient for the nth mode given by the expression in brackets in (41) and are evaluated at $\rho = a$. Equation (44) is in the form of a cosine series in ϕ', so the Fourier series coefficients for the exponential series representation of $f(\phi', t)$ in (13) are easily seen to be

$$f_n = \frac{\varepsilon_n}{2b} \Gamma_n \cos(\omega_a t + \theta_n) \tag{45}$$

where $\varepsilon_0 = 2$ and $\varepsilon_n = 1$ for $n > 0$. Substituting coefficients from (45) into (14) and (30) completes the solution for the time-dependent shape variation for both the TM and TE cases.

Considering the dielectric constant to be a macroscopic material parameter directly related to the dipole moment per unit volume, the relationship between the displacement interior to the cylinder and dielectric constant fluctuation is shown from (61) in the Appendix to be

$$\delta\tilde{\epsilon}(\rho', \phi', t) = -(\epsilon_d - \epsilon_0) \nabla \cdot \mathbf{u}(\rho', \phi', t). \tag{46}$$

Furthermore, the divergence of the displacement vector has a relatively simple form and can be shown using (41) and (42) to be

$$\nabla \cdot \mathbf{u} = \kappa_1^2 \sum_{n=0}^{\infty} a_n J_n(\kappa_1 \rho') \cos n\phi'. \tag{47}$$

Inserting (47) into (46) and expressing the time dependence explicitly gives

$$\delta\tilde{\epsilon}(\rho', \phi', t) = -(\epsilon_d - \epsilon_0)\kappa_1^2 \sum_{n=0}^{\infty} \Upsilon_n(\rho') \cdot \cos(\omega_a t + \gamma_n(\rho')) \cos n\phi' \tag{48}$$

where $\Upsilon_n(\rho')$ and $\gamma_n(\rho')$ are the magnitude and phase, respectively, of $a_n J_n(\kappa_1 \rho')$ in (47). From this expression, it is apparent that the series coefficients for the exponential Fourier series representation of $\tilde{\epsilon}(\rho', \phi', t)$ in ϕ' are

$$\tilde{\epsilon}_n(\rho', t) = -\frac{\varepsilon_n}{2\delta} (\epsilon_d - \epsilon_0)\kappa_1^2 \Upsilon_n(\rho') \cos(\omega_a t + \gamma_n(\rho')) \tag{49}$$

where $\varepsilon_0 = 2$ and $\varepsilon_n = 1$ for $n > 0$. Substituting the Fourier series coefficients from (49) into (23) and (40) completes the solution for the time-varying dielectric fluctuation for both the TM and TE cases.

Note that both the shape variation and dielectric constant fluctuation of the cylinder can be accounted for by expanding the unperturbed scattered fields in a perturbation expansion in terms of both b and δ. The expansions in b and δ can be treated independently since the inclusion of terms containing $b\delta$ are of second order and higher. Hence, the total scattered field including both shape and dielectric fluctuation is estimated by coherently adding the results from the two perturbation expansions described in this paper. Taking the Fourier transform of the time-varying scattered field will provide the desired scattered Doppler spectrum.

III. Simulation and Results

When the frequency of the incident acoustic wave is not close to a mechanical resonance of the cylinder, it behaves as an impenetrable rigid cylinder [24]. Consequently, significant displacement, and thus, a measurable Doppler spectrum only occurs when the incident acoustic frequency corresponds to a resonant mode of the cylinder. To illustrate the Doppler response at resonance, consider a 10 cm radius, solid cylinder composed of polyethylene ($\epsilon_d/\epsilon_0 = 2.25$) illuminated by an incident acoustic plane wave in air with a power density of 1 kW/m^2 at a EM frequency of 3 GHz. The first acoustic resonance, corresponding to the 2nd mode, occurs at an acoustic frequency of $f_a = 2.02$ kHz for a 10 cm radius cylinder. The density of polyethylene is 0.9 g/cm^3, with the velocities of 1950 m/s for the longitudinal acoustic wave and 540 m/s for the transverse (shear) wave [25]. The backscattered Doppler spectrum for a TM incident EM wave is shown in Fig. 3 for the $n = 2$ acoustic resonance where the effects of both surface and dielectric fluctuations are included. The spectrum is discrete since the vibration of the cylinder is periodic, and the first Doppler harmonic occurs at a frequency coincident with the acoustic vibration frequency. This indicates that the frequency of vibration of an object can be determined by the location of the first Doppler harmonic. The vibrating object is essentially modulating the amplitude and phase of the scattered EM wave, thus generating the Doppler spectrum.

A relevant topic to consider at this point is the relative contribution to the Doppler spectrum from the two scattering mechanisms described in this paper. As a comparison, the bi-static scattering with TM incidence of the 1st harmonic of the Doppler spectrum from the cylinder at the acoustic resonance corresponding to $n = 2$ is shown in Fig. 4, where the contribution from the shape deformation and the dielectric fluctuation are shown separately. Similarly, the contribution from each for the $n = 1$ acoustic mode is shown in Fig. 5. From Fig. 4, the shape variation dominates the Doppler scattering for the $n = 2$ mode with the dielectric contribution around 40 dB below that of the shape variation. However, Fig. 5 reveals that for the $n = 1$ mode, both the shape and dielectric variation contributions are of the same order and both must be included to obtain correct results. Note that the shape and dielectric contributions are added *coherently* to obtain the complete result. The bi-static scattering for TE incidence of the 1st

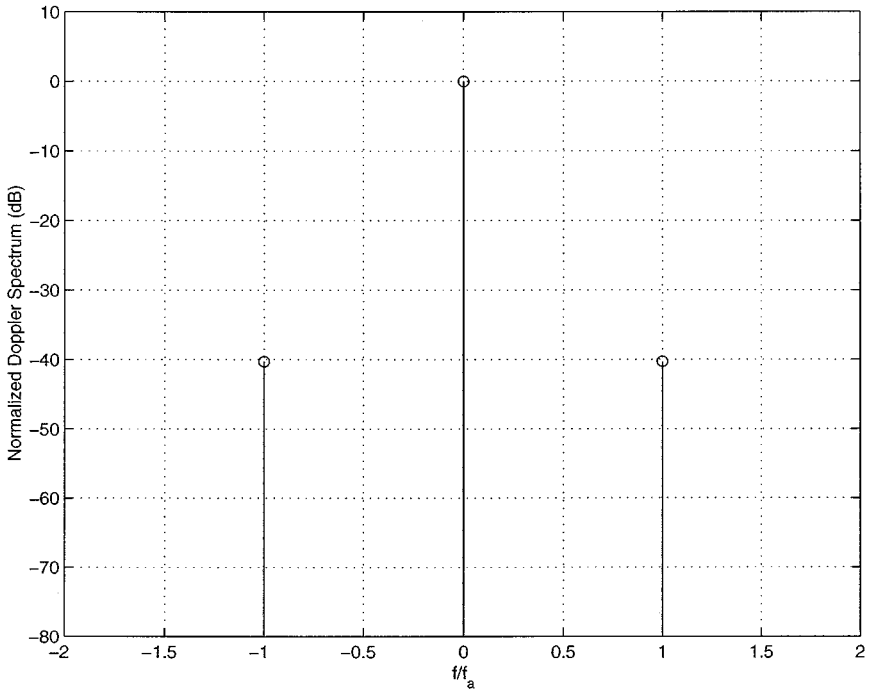

Fig. 3. Backscattered Doppler spectrum for a TM incident plane wave from an acoustically excited, solid polyethylene cylinder with a radius of 10 cm at 3 GHz. The $n = 2$ acoustic resonant mode is excited at an acoustic frequency of 2.02 kHz.

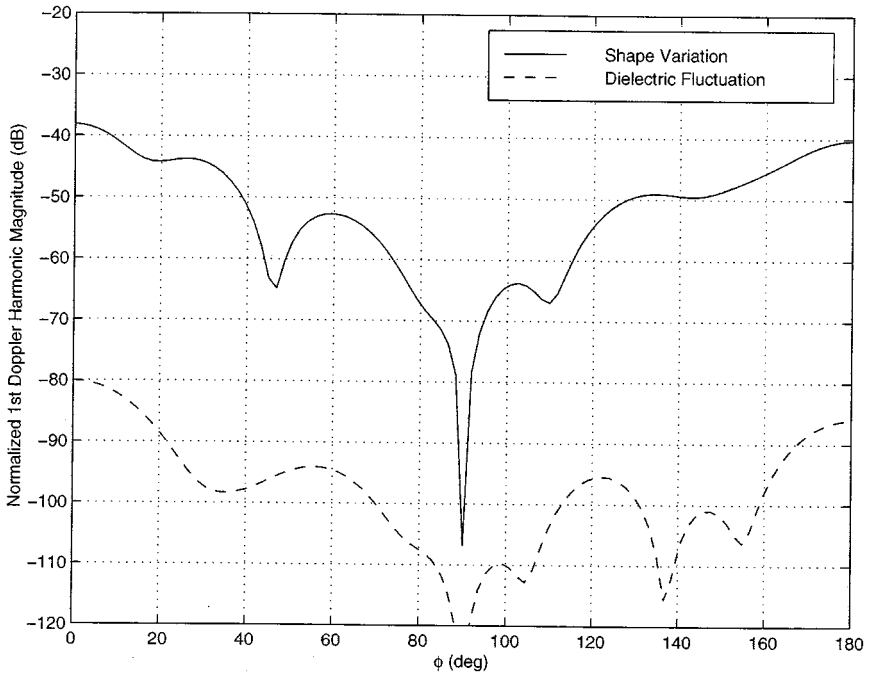

Fig. 4. Bistatic scattering (TM incidence) of the 1st Doppler harmonic showing the relative contribution from the shape and dielectric fluctuations with the $n = 2$ acoustic mode excited.

harmonic of the Doppler spectrum from the cylinder, with both shape and dielectric contributions included, is shown in Fig. 6 for the first two acoustic resonant modes.

To illustrate the effect of acoustic resonance on the scattered Doppler spectrum, the magnitude of the 1st harmonic of the Doppler spectrum is calculated as a function of acoustic frequency and is plotted in Fig. 7 for TM incidence. The magnitude of the 1st Doppler harmonic is highly sensitive to the acoustic resonances of the cylinder. In fact, the magnitude of the Doppler harmonic is negligible except around narrow resonances corresponding to the acoustic resonances of the cylinder. A similar result is observed for solid metallic cylinders in [2]. The first resonance occurs for the $n = 2$ mode followed by the $n = 1$, and $n = 3$ modes. By sweeping acoustic frequency, the mechanical resonances of the cylinder can be determined from the Doppler spectrum. Furthermore, the frequency loca-

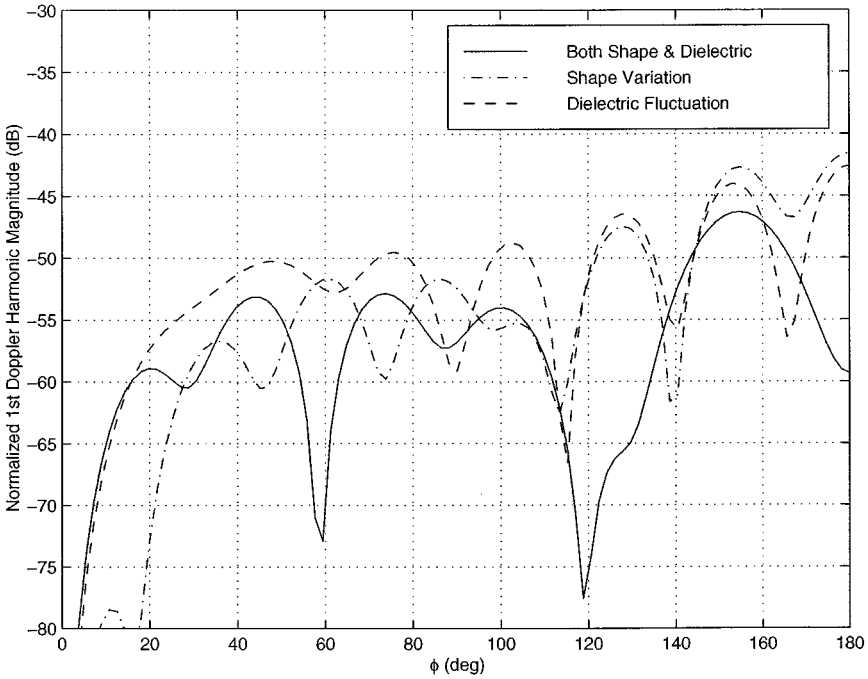

Fig. 5. Bistatic scattering (TM incidence) of the 1st Doppler harmonic showing the relative contribution from the shape and dielectric fluctuations with the $n = 1$ acoustic mode excited. Shape and dielectric contributions are added coherently for the complete result.

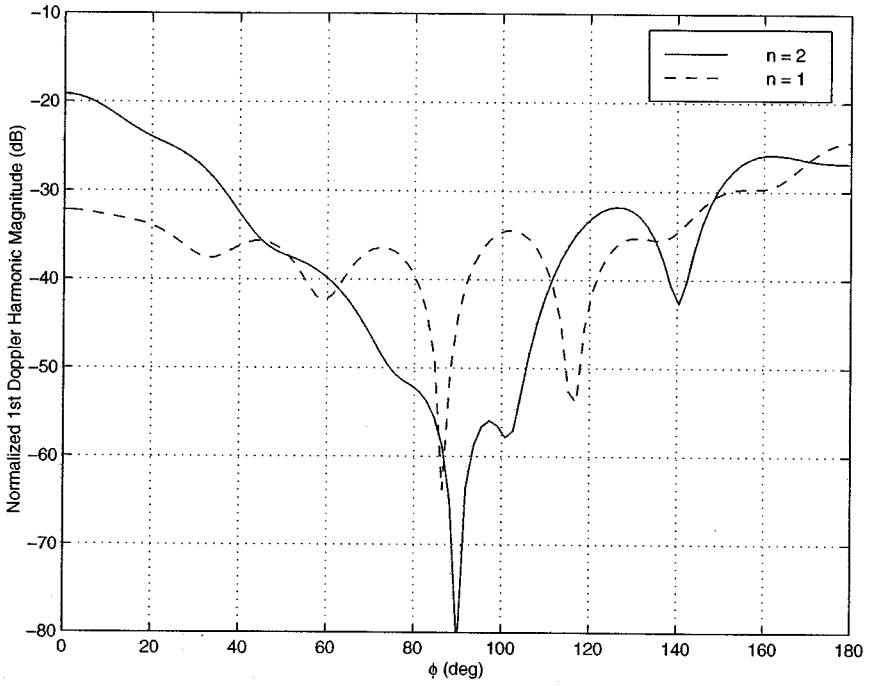

Fig. 6. Variation of the 1st Doppler harmonic magnitude with ϕ for TE incidence with both shape and dielectric fluctuations included. The first two acoustic resonances are shown.

tions of these resonances are independent of the background medium. These results apply to both TM and TE incidence. One should note that a cylinder of different size or material property will have different acoustic resonances. Hence, using the EM Doppler spectrum scattered from an acoustically vibrated object could provide a means of buried object discrimination based on the location and distribution of the resonances in the Doppler response.

Recognizing the sensitivity of the Doppler spectrum to the acoustic resonances, it is natural to question whether the sensitivity is also observed near EM resonances. The frequency location of the EM resonances can be found by solving for the eigenvalues of the unperturbed, homogeneous scattering problem. As an example, consider the TM scattering scenario. By expressing valid solutions to the wave equation both outside and inside the cylinder and enforcing the continuity of the tangential fields at

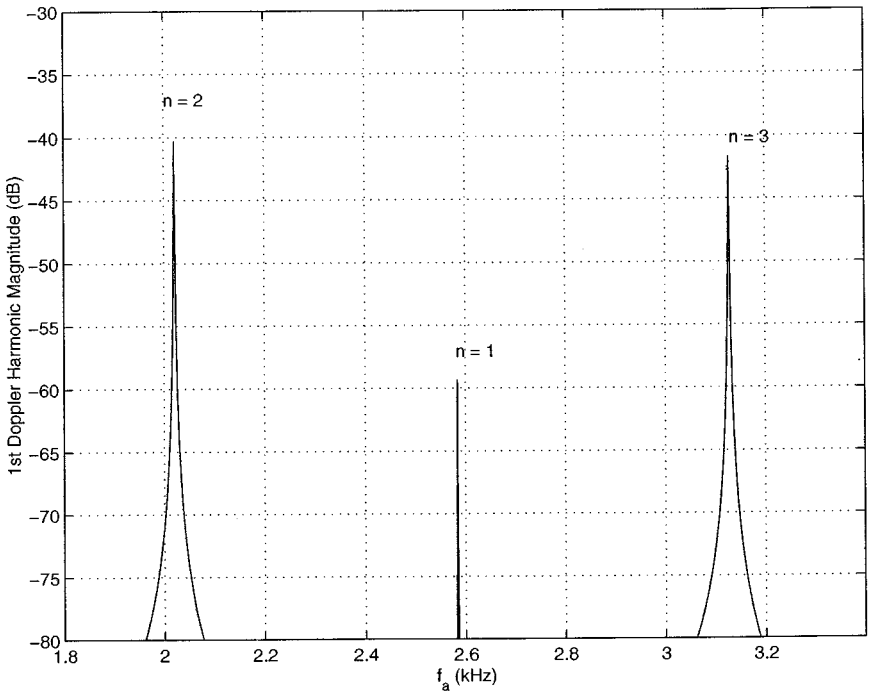

Fig. 7. Variation of the first Doppler harmonic magnitude with acoustic excitation frequency for a TM plane EM wave incident upon a solid polyethylene cylinder.

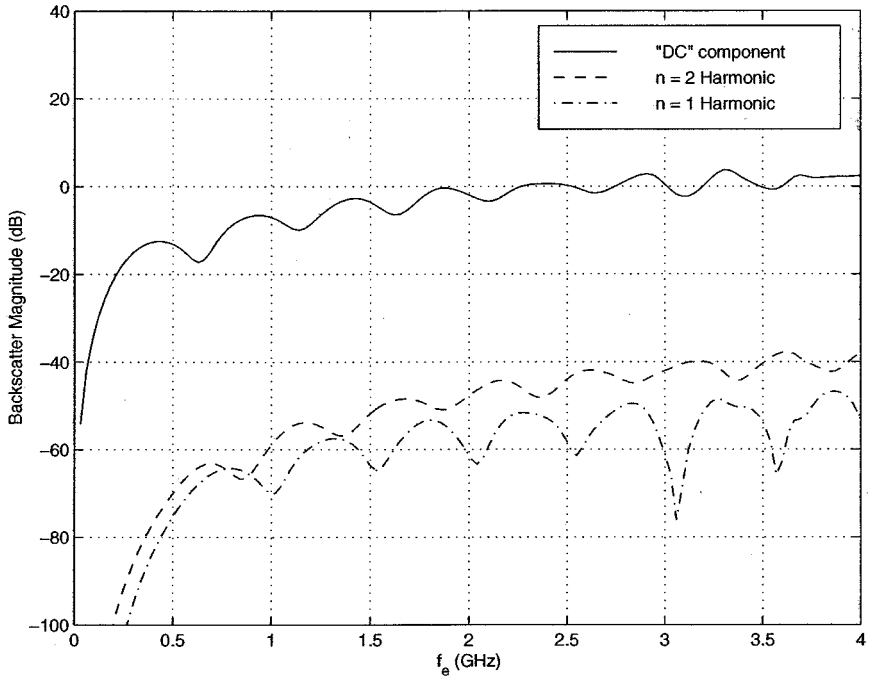

Fig. 8. Variation of the backscattered 1st Doppler harmonic magnitude with EM frequency for TM incidence upon a solid polyethylene cylinder. Both the $n = 1$ and $n = 2$ acoustic modes are excited, and both shape and dielectric contributions are included.

the surface of the cylinder, the determinant of the system can be written

$$J_n(k_d a)H_n^{(2)\prime}(k_0 a) - \frac{\eta_0}{\eta_d} J_n'(k_d a)H_n^{(2)}(k_0 a) = 0. \qquad (50)$$

Roots of this equation represent the resonant frequencies of the system and are generally complex quantities. For dielectric constants close to unity, the roots lie far away from the real axis and the frequency response is not oscillatory. As the dielectric constant increases, the roots of (50) move closer to the real axis with a corresponding increase in oscillation of the frequency response. To illustrate the effect of EM resonance on the scattered field from an acoustically vibrated cylinder, the Doppler response (TM incidence) was calculated for EM frequencies swept from the Rayleigh scattering region through the resonance region and is shown in Fig. 8. For comparison, the unshifted (or "DC") component of the backscattered spectrum is

plotted together with the first Doppler harmonic for both the $n = 1$ and $n = 2$ acoustic modes. The unshifted component corresponds to the scattering from an unperturbed dielectric cylinder. Furthermore, both shape and dielectric contributions to the Doppler are included. From the figure it is seen that the Doppler components of the backscatter undergo oscillations in the resonance region but are not necessarily in phase with the unshifted component. This result is not entirely unexpected since peaks in the unperturbed response are due to the combined effects of multiple roots from (50) and the Doppler components are likewise the result of multiple sources. Similar results have been obtained for TE incidence. If the dielectric constant of the cylinder is increased, the internal fields become more sensitive to resonances, suggesting that the density fluctuations might contribute more to the Doppler scattering. This, however, is not the case. While the internal fields do become more sensitive to resonances with increased dielectric constant, the internal field strength is reduced because coupling from the external source becomes weaker, thus reducing the effect of density fluctuations. Overall, the Doppler response is found to be much more sensitive to the acoustic rather than EM resonances, and a sweep of acoustic frequency is likely to provide better discrimination capability.

IV. Conclusion

In this paper, an analytical formulation for the acousto-electromagnetic scattering behavior of a dielectric cylinder has been developed. Both shape variation and dielectric fluctuations have been shown to contribute to the Doppler spectrum observed in the scattered field. Results indicate that the Doppler response of an acoustically vibrated cylinder is a strong function of scattering angle and highly dependent upon its acoustic resonances. In fact, the only significant Doppler response occurs when the object is excited at an acoustic resonance. Also, the sensitivity of the Doppler response to EM resonances was found to be much less than to acoustic resonances. The phenomenology observed here can be applied to the area of buried object detection and discrimination where a swept frequency acoustic source is used to excite the buried objects and the measured Doppler response is used for detection and identification. To fully extend the results here to buried objects, the scattering from vibrating objects beneath an air-ground interface should be considered and is reserved for future work.

Appendix

The permittivity of a dielectric material under acoustic vibration becomes inhomogeneous as the bulk density of the material becomes a function of position. The dielectric of a material is defined as [26]

$$\epsilon = \frac{\mathbf{D}}{\mathbf{E}} = \frac{\epsilon_0 \mathbf{E} + \mathbf{P}}{\mathbf{E}} \tag{51}$$

where $\mathbf{P}$ is the dipole moment per unit volume. $\mathbf{P}$ is related to the electric susceptibility (χ) by

$$\mathbf{P} = \epsilon_0 \chi \mathbf{E} \tag{52}$$

and

$$\epsilon = \epsilon_0(\chi + 1). \tag{53}$$

The dipole moment per unit volume is related to the number of molecules per unit volume (N) multiplied by the dipole moment of each molecule ($\mathbf{d}$)

$$\mathbf{P} = N\mathbf{d}. \tag{54}$$

Now suppose the mass of each molecule is m, so the material bulk density (ϱ) is given by

$$\varrho = Nm. \tag{55}$$

Condensation $s(\mathbf{r})$ is an acoustic parameter that is related to the bulk density and the displacement vector ($\mathbf{u}$) by [27]

$$s(\mathbf{r}) = \frac{\varrho(\mathbf{r}) - \varrho_0}{\varrho_0} = -\nabla \cdot \mathbf{u}(\mathbf{r}) \tag{56}$$

where ϱ_0 is the unperturbed bulk density of the material. Substituting (55) into (56) we obtain

$$s(\mathbf{r}) = \frac{N(\mathbf{r})m - N_0 m}{N_0 m} = \frac{N(\mathbf{r}) - N_0}{N_0}. \tag{57}$$

Multiplying both numerator and denominator by $\mathbf{d}$

$$s(\mathbf{r}) = \frac{\mathbf{P}(\mathbf{r}) - \mathbf{P}_0}{\mathbf{P}_0} = \frac{\epsilon_0 \chi(\mathbf{r})\mathbf{E} - \epsilon_0 \chi_0 \mathbf{E}}{\epsilon_0 \chi_0 \mathbf{E}} \tag{58}$$

$$= \frac{\epsilon_0(\chi(\mathbf{r}) + 1) - \epsilon_0(\chi_0 + 1)}{\epsilon_0(\chi_0 + 1) - \epsilon_0} \tag{59}$$

$$= \frac{\epsilon(\mathbf{r}) - \epsilon_d}{\epsilon_d - \epsilon_0} \tag{60}$$

where ϵ_d is the dielectric constant for the unperturbed material. Hence, the fluctuating part of the dielectric constant is given by

$$\delta\tilde{\epsilon}(\mathbf{r}) = -(\epsilon_d - \epsilon_0)\nabla \cdot \mathbf{u}(\mathbf{r}). \tag{61}$$

References

[1] C. Bruschini and B. Gros, "A survey of current sensor technology research for the detection of landmines," in *Proc. Int. Workshop Sustainable Humanitarian Demining*, Sept. 29–Oct. 1, 1997, pp. 6.18–6.27.

[2] K. Sarabandi and D. E. Lawrence, "Acoustic and electromagnetic wave interaction: Estimation of Doppler spectrum from an acoustically vibrated metallic circular cylinder," IEEE Trans. Antennas Propagat., Apr. 1999, submitted for publication.

[3] C. Stewart, "Summary of mine detection research," U.S. Army engineering res. and devel. labs, Corps. of Eng., Belvoir, VA, Tech. Rep.1636-TR, vol. I, pp. 172–179, May 1960.

[4] G. S. Smith, "Summary report: Workshop on new directions for electromagnetic detection of nonmetallic mines," Report for U.S. Army BRDEC and ARO, June 1992.

[5] W. R. Scott, Jr. and J. S. Martin, "An experimental model of a acousto-electromagnetic sensor for detecting land mines," in *IEEE AP-S Int. Symp. Dig.*, Atlanta, GA, July 1998, pp. 978–981.

[6] ——, "Experimental investigation of the acousto-electromagnetic sensor for locating land mines," *Proc. of SPIE—Int. Society Optical Engineering*, vol. 3710, no. I, pp. 204–214, 1999.

[7] R. Denier, T. J. Herrick, O. R. Mitchell, D. A. Summers, and D. R. Saylor, "Acoustic and Doppler radar detection of buried land mines using high-pressure water jets," *Proc. of SPIE—Int. Society Optical Engineering*, vol. 3710, no. I, pp. 247–255, August 1999.
[8] D. Wood, Jr., "Hybrid method of moments solution for a perturbed dielectric circular cylinder," *Appl. Comput. Electromagn. Soc. J.*, vol. 10, no. 3, pp. 47–52, Nov. 1995.
[9] L. Rayleigh, *The Theory of Sound*. New York: Dover, 1945, vol. II, p. 89.
[10] J. C. Maxwell, *A Treatise on Electricity and Magnetism*. New York: Dover, 1954, vol. I, p. 220.
[11] S. O. Rice, "Reflection of electromagnetic waves by slightly rough surfaces," in *The Theory of Electromagnetic Waves*, M. Kline, Ed. New York: Intersciences, 1963.
[12] G. S. Agarwal, "Interaction of electromagnetic waves at rough dielectric surfaces," *Phys. Rev. B, Condens. Matter*, vol. 15, pp. 2371–2383, 1977.
[13] P. C. Clemmow and V. H. Weston, "Diffraction of a plane wave by an almost circular cylinder," *Proc. Roy. Soc. London*, ser. A, vol. 264, p. 246, 1961.
[14] C. Yeh, "Perturbation method in the diffraction of electromagnetic waves by arbitrary shaped penetrable objects," *J. Math. Phys.*, vol. 6, no. 12, pp. 2008–2013, Dec. 1965.
[15] K. M. Mitzner, "Effect of small irregularities on electromagnetic scattering from an interface of arbitrary shape," *J. Math. Phys.*, vol. 5, no. 12, pp. 1776–1786, Dec. 1964.
[16] C. Yeh, "Perturbation approach to diffraction of electromagnetic waves by arbitrarily shaped dielectric obstacles," *Phys. Rev. A, Gen. Phys.*, vol. 135, p. 1193, 1964.
[17] M. L. Burrows, "A reformulated boundary perturbation theory in electromagnetism and its application to a sphere," *Can. J. Phys.*, vol. 45, pp. 1729–1743, 1967.
[18] P. M. Morse and H. Feshbach, *Methods of Theoretical Physics*. New York: McGraw-Hill, 1953, pt. II, pp. 1073–1078.
[19] K. Sarabandi and T. C. Chiu, "Electromagnetic scattering from slightly rough surfaces with an inhomogeneous dielectric profile," *IEEE Trans. Antennas Propagat.*, vol. 45, pp. 1419–1430, Sept. 1997.
[20] Q. A. Naqvi and A. A. Rizvi, "Low contrast circular cylinder buried in a grounded dielectric layer," *J. Electromagnetic Waves Appl.*, vol. 12, pp. 1527–1536, 1998.
[21] R. F. Harrington, *Time-Harmonic Electromagnetic Fields*, New York: McGraw-Hill, 1961.
[22] C. T. Tai, *Dyadic Green Functions in Electromagnetic Theory*, 2nd ed. New York: IEEE Press, , 1994, pp. 154–158.
[23] J. J. Faran, "Sound scattering by solid cylinders and spheres," *J. Acoust. Soc. Amer.*, vol. 23, no. 4, pp. 405–418, July 1951.
[24] W. P. Mason and R. N. Thurston, *Physical Acoustics Principles and Methods*. New York: Academic, 1981, vol. XV, pp. 191–202.
[25] D. R. Lide, *CRC Handbook of Chemistry and Physics*, 71st ed. Boca Raton, FL: CRC, 1990, pp. 14–32.
[26] W. H. Hayt, Jr., *Engineering Electromagnetics*, 2nd ed. New York: McGraw-Hill, 1967.
[27] L. E. Kinsler, A. R. Frey, A. B. Coppens, and J. V. Sanders, *Fundamentals of Acoustics*, 3rd ed. New York: Wiley, 1982.

Daniel E. Lawrence (S'96) was born in Silver Spring, MD, on June 8, 1973. He received the B.E.E. degree and M.S. degrees in electrical engineering from Auburn University, AL, in 1996 and 1998, respectively. He is currently working toward the Ph.D. degree in the Radiation Laboratory at the University of Michigan, Ann Arbor.

From 1997 to 2000, he was a DoD Graduate Research Fellow investigating the use of low-frequency magnetic fields for buried landmine discrimination. He has also performed analytical analysis of acousto-electromagnetic methods applied to buried object detection. His current research interests include microwave and millimeter-wave radar systems, techniques used in buried landmine detection/identification, and the interaction of acoustic and electromagnetic waves.

Kamal Sarabandi (S'87–M'90–SM'92–F'00) received the B.S. degree in electrical engineering from Sharif University of Technology, Tehran, Iran, in 1980. He received the M.S.E. degree in electrical engineering in 1986, the M.S. degree in mathematics and the Ph.D. degree in electrical engineering in 1989, from the University of Michigan, Ann Arbor.

Currently, he is with the University of Michigan as Director of the Radiation Laboratory and Associate Professor in the Department of Electrical Engineering and Computer Science. He has served as the Principal Investigator on many projects sponsored by NASA, JPL, ARO, ONR, ARL, NSF, DARPA and numerous industries. He has published numerous book chapters and over 90 papers in journals on electromagnetic scattering, random media modeling, wave propagation, antennas, microwave measurement techniques, radar calibration, inverse scattering problems, and microwave sensors. He has over 170 papers and invited presentations in national and international conferences and symposia. His research interests include electromagnetic wave propagation, antennas, and microwave and millimeter-wave radar remote sensing.

Dr. Sarabandi is a member of the IEEE Geoscience and Remote Sensing Society (GRSS) ADCOM, chairman of the Awards Committee of the IEEE GRSS, and a member of IEEE Technical Activities Board Awards Committee. He is serving as the Associate Editor of the IEEE TRANSACTIONS ON ANTENNAS AND PROPAGATION and the IEEE SENSORS JOURNAL. He is a member of Commission F of URSI and of The Electromagnetic Academy. He is listed in American Men and Women of Science and Who's Who in Electromagnetics. He was the recipient of the prestigious Henry Russel Award from the Regents of The University of Michigan (the highest honor the University of Michigan bestows on a faculty member at the assistant or associate level). In 1999, he received a GAAC Distinguished Lecturer Award from the German Federal Ministry for Education, Science, and Technology. In 1996, he was a recipient of a 1996 Teaching Excellence Award from the EELS Department of The University of Michigan.